A Texture Analysis Approach for Characterizing Microcalcifications on Mammograms

Anna N. Karahaliou, Ioannis S. Boniatis, Spyros G. Skiadopoulos, Filippos N. Sakellaropoulos, Eleni Likaki, George S. Panayiotakis and Lena I. Costaridou*

***Abstract*—The current study investigates whether texture properties of the tissue surrounding microcalcification (MC) clusters can contribute to breast cancer diagnosis. The case sample analyzed consists of 100 mammographic images, originating from the Digital Database for Screening Mammography (DDSM). All mammograms selected correspond to heterogeneously and extremely dense breast parenchyma and contain subtle MC clusters (46 benign and 54 malignant, according to database ground truth tables). Regions of interest (ROIs) of 128x128 pixels, containing the MCs are used for the subsequent texture analysis. ROIs are preprocessed using a wavelet-based locally adapted contrast enhancement method and a thresholding technique is applied to exclude MCs. Texture features are extracted from the remaining ROI area (surrounding tissue) employing first and second order statistics algorithms, grey level run length matrices and Laws' texture energy measures. Differentiation between malignant and benign MCs is performed using a k-nearest neighbour (kNN) classifier and employing the leave-one-out training-testing methodology. The Laws' texture energy measures demonstrated the highest performance achieving an overall accuracy of 89%, sensitivity 90.74% (49 of 54 malignant cases classified correctly) and specificity 86.96% (40 of the 46 benign cases classified correctly). Texture analysis of the tissue surrounding MCs shows promising results in computer-aided diagnosis of breast cancer and may contribute to the reduction of benign biopsies**.

I. Introduction

MAMMOGRAPHY is currently the most effective imaging modality for breast cancer screening. However, the sensitivity of mammography is highly challenged by the presence of dense breast parenchyma, which deteriorates both detection and characterization tasks [1], [2]. Computer Aided (CA) detection systems have been developed to aid radiologists in detecting mammographic lesions, characterized by promising performance [3]-[6]. CA diagnosis/characterization systems for aiding the decision concerning biopsy and follow-up are still under development [1].

Various CA diagnosis algorithms have been proposed for the characterization of microcalcifications (MCs), an important indicator of malignancy. These algorithms are based on extracting image features from regions of interest (ROIs) and estimating the probability of malignancy for a given MC cluster. A variety of computer-extracted features and classification schemes have been used to automatically discriminate between benign and malignant MC clusters. The majority of these studies have followed two approaches.

The first approach is based on computer extracted morphology/shape features of individual MCs or of MC clusters [7]-[16], since morphology is one of the most important clinical factors in breast cancer diagnosis. CAD schemes that employ the radiologists' ratings of MCs morphology have also been proposed [17-19]. The second approach employs texture features extracted from ROIs containing MC clusters [9], [20]-[24].

Some studies have compared morphological vs. textural features but the results are differentiated with respect to the features investigated, the classifiers used and datasets analyzed. A combination of both morphological and textural features has also been studied, providing promising results in breast cancer diagnosis [9], [24].

The highest performance achieved up to now (in terms of area under receiver operating characteristic curve, A_z= 0.98), has been reported by a morphological analysis of MCs also incorporating age in the classification scheme [15]. However, the reproducibility of such schemes depends on the robustness of the MC segmentation algorithm. Furthermore, in case of dense breast parenchyma abutting MCs, the classification task is being highly deteriorated resulting in low specificity values and thus in unnecessary biopsies [1], [2].

The texture analysis approach seems to overcome this limitation since no segmentation stage is required. The rationale of using texture features is based on capturing changes in the texture of the tissue surrounding the MCs. Most texture-based classification studies include MCs in the regions to be further analyzed; however, this rationale introduces bias since the MC, a tiny deposit of calcium in breast tissue, can neither be malignant nor benign. The tissue surrounding or underlying the MC can be malignant or

Manuscript received June 30, 2006. This work was supported by the European Social Fund (ESF), Operational Program for Educational and Vocational Training II (EPEAEK II), and particularly the Program PYTHAGORAS I (B.365.011). *Asterisk indicates corresponding author.*

*L. I. Costaridou is with the Department of Medical Physics, School of Medicine, University of Patras, 265 00 Patras, Greece (+30-2610-969111; fax: +30-2610-996113; e-mail: costarid@upatras.gr).

A. N. Karahaliou, I. S. Boniatis, S. G. Skiadopoulos and F. N. Sakellaropoulos are with the Department of Medical Physics, School of Medicine, University of Patras, 265 00 Patras, Greece (email: karahaliou.a@med.upatras.gr; iboniat@in.gr; skiado@med.upatras.gr; phisakel@med.upatras.gr).

E. Likaki is with the Department of Radiology, School of Medicine, University of Patras, 265 00 Patras, Greece (e-mail: likaki@med.upatras.gr).

G. S. Panayiotakis is with the Department of Medical Physics, School of Medicine, University of Patras, 265 00 Patras, Greece, and also with the Medical Radiation Physics Unit, University Hospital of Patras, 265 00 Patras, Greece (e-mail: panayiot@upatras.gr).

benign. This tissue is also the one subjected to pathoanatomical and immunochemistry analysis to derive a benign or malignant outcome.

To the best of the authors' knowledge, there is only one study based on texture analysis of the tissue surrounding MCs for breast cancer diagnosis [25]. This study used a dataset of 54 scout views acquired from digital stereotactic equipment before needle insertion. Textural features extracted are based on co-occurrence matrices and fractal geometry. Classification was performed with Linear and Logistic Discriminant analysis. Their work has successfully validated the hypothesis that tissue surrounding MCs can be used for breast cancer diagnosis.

The current study investigates whether texture properties of the tissue surrounding MC clusters on screening mammograms can be used for breast cancer diagnosis thus, providing to radiologist an estimation of malignancy prior to the biopsy procedure. Mammograms of high breast density were selected since the presence of dense breast parenchyma deteriorates the characterization task of MC clusters and yields low specificity values [1].

The steps of the proposed method are illustrated in Figure 1.

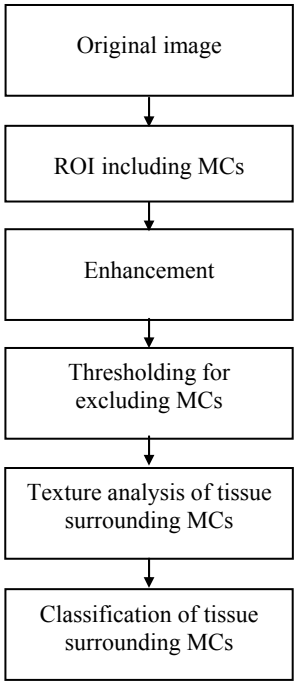

Fig. 1. Flowchart of the preprocessing and classification task performed in this study.

II. Material and Methods

A. Case Sample

The case sample consists of 100 mammographic images originating from the Digital Database for Screening Mammography (DDSM) [26], digitized with the LUMISYS 300 scanner at 12-bit pixel depth and spatial resolution 50 μm. All mammograms selected contain MC clusters (46 benign and 54 malignant, according to database ground truth tables) and correspond to heterogeneously dense and extremely dense breast parenchyma (density 3 and 4 according to the ACR BIRADS^{TM} lexicon [27]).

B. Enhancement

Images are preprocessed using a wavelet-based spatially adaptive method for mammographic contrast enhancement [28], [29]. This method is selected since it has shown high performance in enhancing MCs as compared to other enhancement methods proposed for mammographic enhancement [30]. The method is based on local modification of multiscale gradient magnitude values provided by the redundant dyadic discrete wavelet transform. Specifically, a denoising process is firstly performed taking into account local signal in breast area and noise standard deviation estimated in the mammogram background. Contrast enhancement is accomplished by applying a local linear mapping operator on denoised wavelet gradient magnitude values; coefficient mapping is controlled by a local gain limit parameter. The processed image is derived by reconstruction from the modified wavelet coefficients. Preprocessing was performed on rectangular 600x600 pixels ROIs containing the MCs instead of the whole image to reduce calculation time. Figure 2 presents a ROI of 600x600 pixels containing the MC cluster in original image (a) and the corresponding processed ROI (b).

C. Thresholding for Excluding MCs

An experienced radiologist defined manually a ROI_{rad} containing the MCs on each processed 600x600 ROI. To avoid high grey level value pixels corresponding to normal tissue identified as MCs, a simple thresholding algorithm was empirically applied on ROI_{rad} to exclude MCs (fig. 2c). The resulting binary image produced is shown in figure 2(d). By reversing the binary image and multiplying with the original 600x600 ROI the resulted image ROI, named surrounding tissue ROI (ST-ROI) provided in fig. 2(e), is similar to the original one without MCs. The use of most robust segmentation technique was not deemed necessary for the aim of this study, since neither morphology analysis of individual MCs nor of MC clusters is performed.

D. Texture Analysis of Tissue Surrounding MCs

Texture analysis is performed in a 128x128 pixels subregion of each ST-ROI (fig. 2f). Specifically, the 128x128 pixels ROI was placed in such a way to contain the cluster at its center. Most of the clusters in the dataset analyzed could be contained within a 128x128 ROI. For the clusters that are substantially larger than a single ROI, additional ROIs containing the remaining parts of the cluster are defined and processed in the same way as the other ROIs. The texture feature values extracted from the different ROIs of the same cluster are averaged and the average values are used as the feature values for that cluster.

In this study four categories of textural features are extracted: First Order Statistics (FOS), Grey Level Co-

occurrence Matrices (GLCM), Grey Level Run Length Matrices (GLRLM) and Law's Texture Energy Measures (LTEM).

1) First Order Statistics Features: FOS provides different statistical properties (4 statistical moments) of the intensity histogram of an image [31]. They depend only on individual pixel values and not on the interaction or co-occurrence of neighboring pixel values. In this study, four first order textural features were calculated: Mean value of gray levels (1), Standard Deviation of gray levels (2), Kurtosis (3) and Skewness (4).

2) Grey Level Co-occurrence Matrix Features: The GLCM is a well-established robust statistical tool for extracting second order texture information from images [32], [33]. The GLCM characterizes the spatial distribution of gray levels in the selected ST-ROI subregion. An element at location (i,j) of the GLCM signifies the joint probability density of the occurrence of gray levels i and j in a specified orientation θ and specified distance d from each other. Thus, for different θ and d values, different GLCMs are generated. In this study, four GLCMs corresponding to four different directions (θ=0°, 45°, 90° and 135°) and one distance (d=1 pixel), were computed for each selected ST-ROI subregion. Thirteen features were derived from each GLCM. Specifically, the features studied are: Energy, Entropy, Contrast, Local Homogeneity, Correlation, Shade, Promenance, Sum of Squares, Sum Average, Sum Entropy, Difference Entropy, Sum Variance and Difference Variance. Four values were obtained for each feature corresponding to the four matrices. The mean (M) and range (R) of these four values were calculated, comprising a total of twenty-six second order textural features.

3) Gray Level Run Length Matrix Features: The GLRLM provides information related to the spatial distribution of gray level runs (i.e. pixel-structures of same pixel value) within the image [34]. Textural features extracted from GLRLM evaluate the distribution of small (short runs) or large (long runs) organized structures within ST-ROI subregion. From each ST-ROI subregion, five run-length features were generated: Short Runs Emphasis (SRE), Long Runs Emphasis (LRE), Grey Level Non-Uniformity (GLNU), Run Length Non-Uniformity (RLNU) and Run Percentage (RPERC). Four values were computed for each feature, corresponding to the angles of 0, 45, 90 and 135◦. The mean (M) and range (R) of these four values were calculated, comprising a total of 10 features.

4) Laws' Texture Energy Measure Features: According to the method proposed by Laws, textural features were extracted from images that had been previously filtered by each one of the 25 Laws' masks or kernels [35]. These filtered images were characterized as Texture Energy images (TE images). Averaging the filtered images corresponding to symmetrical kernels (such as R5L5 and L5R5), and taking into account that 20 out of 25 kernels are symmetric one to each other, 15 TR images were produced. From each 1 of the 15 TR images, 5 first-order statistics (mean, standard deviation, range, skewness and kurtosis) were computed, giving in total 75 Laws' textural features: 5 sets of 15 features each, with each 15-feature set corresponding to each one of the 5 first-order statistics, i.e. 15 features for the Mean value (M), 15 features for the Standard deviation (STD), 15 for the Range (R), 15 for the Skewness (S) and 15 for the Kurtosis (K).

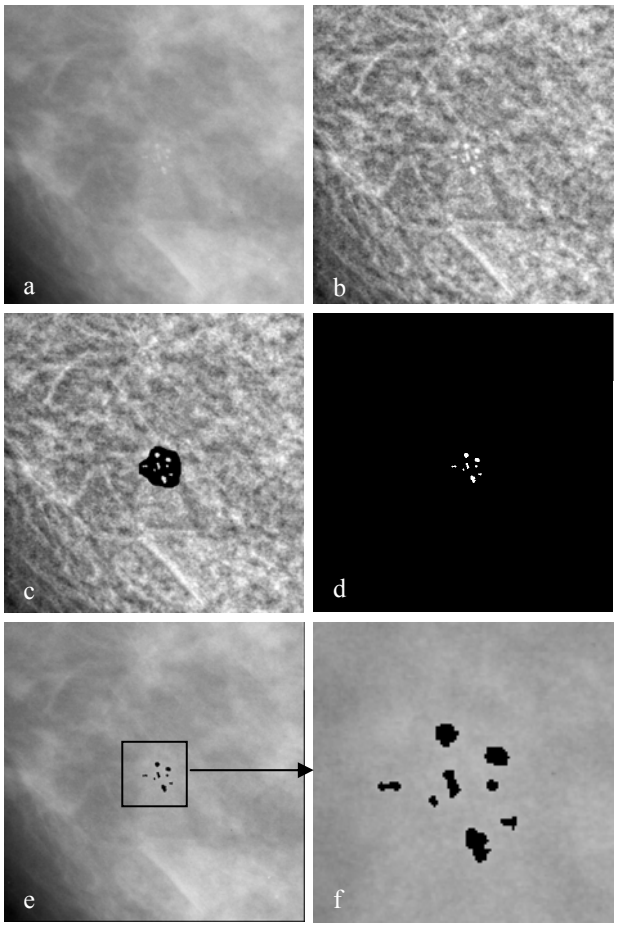

Fig. 2. (a) 600x600 pixels ROI containing a malignant MC cluster in original mammogram (DDSM: B_3406_RIGHT_CC), (b) processed ROI, (c) binarization on manually defined ROI, (d) binarized MC cluster on 600x600 pixels ROI, (e) surrounding tissue ROI (ST-ROI), (f) magnified 128x128 pixels subregion of ST-ROI.

E. Classification of Tissue Surrounding MCs

A k-nearest neighbor (kNN) classifier was used for the classification of tissue surrounding MCs. kNN makes a class assignment based on the classes of the k training samples nearest to the test/unknown sample. In this study, the inverse distance-weighted voting was used [36]. In this approach, closer neighbors get higher votes.

Specifically, the vote of the k^{th} neighbor is defined as:

$$vote(k) = \frac{1}{d_k + 1} \quad (1)$$

where d_k is the Euclidean distance of the k^{th} neighbor from the test sample. The votes of each class are summed and the test sample is assigned to class with the highest sum of

votes. Specifically, the *Decision* function for classification is given by:

$$Decision = \sum_{i=0}^{n} vote(i)_{classA} - \sum_{j=0}^{m} vote(j)_{classB} \quad (2)$$

where n and m are integers ranging from 0 up to k, satisfying the equation $n+m=k$. In this study, k ranged from 1 up to 31 neighbors. If *Decision* is greater than zero, the test sample is assigned to class A (malignant); otherwise, the test sample is assigned to class B (benign).

Feature selection was performed by means of exhaustive search. Best subset of features was selected with respect to maximum accuracy achieved. The training and testing of the classifier was performed using the leave-one-out methodology. Specifically, all cases of the sample were tested. When the λ^{th} case was being tested the training set consisted of all cases except from the λ^{th} case.

The four categories of textural features were tested separately and the performance of the classifier for each textural features category was evaluated by means of sensitivity, specificity and overall classification accuracy.

III. Results

Table I summarizes the results of the classification performance of the four categories of textural features investigated, in terms of sensitivity, specificity and overall accuracy.

The Laws' Texture Energy Measures demonstrated the highest performance with respect to overall accuracy (89%); high specificity was achieved (86.96%) while maintaining high sensitivity (90.74%). Co-occurrence matrices features provided a sufficient classification performance (82% accuracy). This category of features have been previously used for breast cancer diagnosis, extracted from ROIs containing [9], [20], [21], [24] or excluding [25] the MCs, demonstrating a comparable performance. First order statistics provided an overall accuracy of 79% with high sensitivity (92.59%). The fact that Ductal Carcinoma in Situ (DCIS) occurs overwhelmingly in the mammographically dense areas of the breast [37], justifies the inclusion of Mean grey level value in the best feature set of the First order statistics. The Run Length matrices features cannot efficiently distinguish malignant from benign MCs (63% accuracy).

IV. Discussion and Conclusions

In this study, a texture analysis approach for breast cancer diagnosis is presented. The method is based on the analysis of the tissue surrounding the MC cluster for prediction of malignancy. This hypothesis has been motivated by the fact that a MC cluster (tiny deposits of calcium in breast tissue) can neither be malignant nor benign. This characterization corresponds to the tissue surrounding and underlying the MC cluster. Furthermore, this tissue is the one subjected to pathoanatomical analysis to be further characterized as malignant or benign.

A similar study has been previously reported by Thiele *et al.* [25], analyzing the surrounding tissue as depicted on scout views from the stereotactic procedure; they achieved a sensitivity of 89% and specificity of 83% in a dataset of 54 cases. In this study we analyzed the surrounding tissue as depicted on screening mammograms, in order to provide to radiologist an aid for estimation of malignancy, prior to the biopsy procedure. Texture analysis was performed on small ROIs (128x128 pixels), where the MCs have been previously excluded, to ensure that the tissue being analyzed is the one subjected to pathoanatomical analysis. Four categories of textural features were investigated, with the Laws' texture energy measures providing the highest classification performance.

While a direct comparison with other texture based classification studies is not possible due to different classification algorithms, textural features and datasets (MC clusters subtlety and breast density types) used, the performance attained by the proposed method is comparable to the performance of the following reported studies.

Dhawhan *et al.* [20] used second order histogram-based features and wavelet-based features extracted from ROIs containing the MCs, and obtained an area under ROC curve (A_z) 0.86 for classification of 191 'difficult-to-diagnose' cases. Chan *et al.* [21] used co-occurrence matrices-based features extracted from ROIs including the MC cluster and achieved an A_z=0.84 in a dataset of 145 cases; when combined both textural and morphological features they achieved an A_z=0.89, which increased to 0.93 when averaging discriminant score from all views of the same cluster (100% sensitivity with 50% specificity). Kramer and Aghdasi [22] used multiscale statistical texture signatures (based on the co-occurrence matrix), as well as wavelet-based texture signatures from ROIs containing the MCs, and compared the performance of both a kNN and a neural network classifier; the neural network perform best achieving a 94.8% overall classification accuracy. Santo *et al.* [23] combined the output of two classifiers for classification of MCs. The first classifier used shape and texture features of individual MCs and the second one used features characterizing the cluster. Their multiple expert system achieved sensitivity 75.7% and specificity 73.5% (A_z =0.79) on a database of 40 mammograms. Zadeh *et al.* [24] compared the performance of four feature sets: texture features (co-occurrence matrices-based) extracted from individual MCs and ROIs containing the cluster, shape quantifiers of MCs, wavelet and multi-wavelet features; the multi-wavelet features outperformed the other methods achieving an A_z=0.89.

The rest of the MCs computer diagnosis algorithms, reported in the literature, have focused on morphology analysis of individual MCs and MC clusters. Comprehensive reviews can be found elsewhere [38], [39], however, some representative studies are provided below for comparison purposes.

Shen *et al.* [7] developed a set of shape features of individual MCs, achieving 100% overall accuracy in classification of 143 individual MCs. Yiang *et al.* [8] used 8 features of MC clusters in a neural network classifier, and

achieved an A_z =0.92 in a dataset of 53 patients. Veldkapm *et al.* [11] used cluster distribution, shape and location features for classification of MCs. A patient-based classification was performed by combining information of both views (MLO and CC), achieving a value of A_z 0.83. Leichter *et al.* [12] used features that reflect the internal architecture within a MC cluster and stepwise discriminant analysis for optimum feature selection and classification. Their approach achieved an A_z=0.98. Verma and Zakos [13] developed a computer-aided diagnosis system for digital mammograms based on fuzzy neural and feature extraction techniques. They used a fuzzy technique to detect microcalcification patterns and a neural network to classify them. Their work achieved a classification rate of 88.9% for classifying the microcalcification as benign or malignant. Lee *et al.* [14] designed a shape recognition-based neural network for capturing geometric information of MCs. They achieved sensitivity 86.1% and specificity 71.4% in a dataset of 40 mammograms. Papadopoulos *et al.* [16] used features characterizing individual MCs and MC clusters; they employed a rule-based system, an artificial neural-network and a support vector machine for classification of MC clusters and achieved an A_z=0.81.

As compared to the morphology-based studies, the proposed method performs within the reported ranges. However, we should note that the feasibility of the proposed texture-based classification scheme was demonstrated on a difficult dataset since all mammograms analyzed correspond to heterogeneously dense and extremely dense breast parenchyma. On the other hand, the success of the various morphology-based classification schemes depends strongly on the robustness of the segmentation algorithm [1], [40], [41]. Especially in case of dense breast parenchyma abutting the MCs, classification is a challenging task due to difficulty induced in the segmentation process. The proposed method by requiring a coarse rather than an accurate segmentation of individual MCs, seems to overcome the limitation of dense breast parenchyma.

In conclusion, the proposed method has shown promising results suggesting that texture analysis of tissue surrounding MC clusters can contribute to computer-aided diagnosis of breast cancer. Completion of the proposed method should include a larger dataset and investigation of additional classification schemes as well as textural features (wavelet and multi-wavelet). Validation of the hypothesis of the surrounding tissue texture analysis will be accomplished by investigating the correlation between computer extracted textural features and pathoanatomical findings.

ACKNOWLEDGMENT

This work is supported by the European Social Fund (ESF), Operational Program for Educational and Vocational Training II (EPEAEK II), and particularly the Program PYTHAGORAS I (B.365.011). We also wish to thank the staff of the Department of Radiology at the University Hospital of Patras for their contribution in this work.

REFERENCES

[1] P. M. Sampat, M. K. Markey, and A. C. Bovik, "Computer-aided detection and diagnosis in mammography" in *Handbook of Image and Video Processing*, 2nd ed., A. C. Bovik Ed. Academic Press, 2005, pp. 1195-1217.

[2] D. D. Adler and M. A. Helvie, "Mammographic biopsy recommendations", *Curr. Opin. Radiol*., vol 4., pp. 123-129, 1992.

[3] M. L. Giger, N. Karssemeijer and S. G. Armato, "Computer-aided diagnosis in medical imaging", *IEEE Trans. on Med. Imaging*, vol. 20, pp. 1205-1208, 2001.

[4] M. L. Giger, "Computer-aided diagnosis of breast lesions in medical images", *Comput. Science Engineering*, vol. 2, pp. 39-45, 2000.

[5] K. Doi, H. MacMahon, S. Katsuragawa, R. M. Nishikawa and Y. Jiang, "Computer-aided diagnosis in radiology: potential and pitfalls", *Eur. J. Radiol*., vol. 31, pp. 97-109, 1999.

[6] C. J. Vyborny, M. L. Giger and R. M. Nishikawa, "Computer-aided detection and diagnosis of breast cancer", *Radiologic Clinics of North America*, vol. 38, pp. 725-740, 2000.

[7] L. Shen, R. M. Rangayyan and J. E. L. Desautels, "Application of shape analysis to mammographic calcifications", *IEEE Trans. Med. Imaging*, vol. 13, pp. 263-274, 1994.

[8] Y. Jiang, R. M. Nishikawa, D. E. Wolverton, C. E. Metz, M. L. Giger, R. A. Schmidt *et al*., "Malignant and benign clustered microcalcifications: automated feature analysis and classification", *Radiology* , vol. 198, pp. 671-678, 1996.

[9] H. P. Chan, B. Sahiner, K. L. Lam, N. Petrick, M. A. Helvie, M. M. Goodsitt and D. D. Adler, "Computerized analysis of mammographic microcalcifications in morphological and texture feature spaces", *Med. Phys.*, vol. 25, pp. 2007-2019, 1998.

[10] O. Tsujii, M. T. Freedman and S. K. Mun, "Classification of microcalcifications in digital mammograms using trend-oriented radial basis function neural network", *Pattern Recognition*, vol. 32, pp. 891-903, 1999.

[11] W. J. H. Veldkamp, N. Karssemeijer, J. D. M. Otten and J. H. C. L. Hendriks, "Automated classification of clustered microcalcifications into malignant and benign types", *Med. Phys.*, vol. 27, pp. 2600-2608, 2000.

[12] I. Leichter, R. Lederman, S. Buchbinder, P. Bamberger, B. Novak, S. Fields, "Optimizing parameters for computer-aided diagnosis of microcalcifications at mammography", *Acad. Radiol.*, vol. 7, pp. 406-412, 2000.

[13] B. Verma, J. Zakos, "A computer-aided diagnosis system for digital mammograms based on fuzzy-neural and feature extraction techniques", *IEEE Trans. Inform. Technol. Biomed.*, vol. 5, pp. 46-54, 2001.

[14] S. K. Lee, P. Chung, C. I. Chang, C. S. Lo, T. Lee, G. C. Hsu, C. W Yang, "Classification of clustered microcalcifications using a Shape Cognitron neural network", *Neural Netw.*, vol. 16, pp. 121-132, 2003.

[15] M. Kallergi, "Computer-aided diagnosis of mammographic microcalcification clusters", *Med Phys*. vol. 31, pp. 314-326, 2004.

[16] A. Papadopoulos, D. I. Fotiadis and A. Likas, "Characterization of clustered microcalcifications in digitized mammograms using neural networks and support vector machines", *Artif. Intell. Med.,* vol. 34, pp. 141-150, 2005.

[17] L. V. Ackerman, A. N. Mucciardi, E. E. Gose and F. S. Alcorn, "Classification of benign and malignant breast tumors on the basis of 36 radiographic properties", *Cancer,* vol. 31, pp. 342–352, 1973.

[18] J. A. Baker, P. J. Kornguth, J. Y. Lo and C. E. Floyd, "Artificial neural network: improving the quality of breast biopsy recommendations", *Radiology*, vol. 198, pp. 131-135, 1996.

[19] Y. Wu, M. L. Giger, K. Doi, C. J. Vyborny, R. A. Schmidt and C. E. Metz, "Artificial neural networks in mammography: application to decision making in the diagnosis of breast cancer", *Radiology*, vol. 187, pp. 81-87, 1993.

[20] A. P. Dhawan, Y. Chitre, and C. Kaiser-Bonasso, "Analysis of mammographic microcalcifications using gray-level image structure features", *IEEE Trans. Med. Imaging*, vol. 15, pp. 246-259, 1996.

[21] H. P. Chan, B. Sahiner, N. Petrick, M. A. Helvie, K. L. Lam, D. D. Adler and M. M. Goodsitt, "Computerized classification of malignant and benign microcalcifications on mammograms: texture analysis using an artificial neural network", *Phys. Med. Biol*., vol. 42, pp. 549-567, 1997.

[22] D. Kramer, F. Aghdasi, "Texture analysis techniques for the classifcation of microcalcifcations in digitized mammograms", in *Proc. 5th IEEE AFRICON Conference Electrotechnical Service for Africa*, Cape Town, 1999, pp. 395-400.
[23] M. De Santo, M. Molinara, F. Tortorella and M. Vento, "Automatic classification of clustered microcalcifications by a multiple expert system", *Pattern Recognition*, vol. 36, pp. 1467-1477, 2003.
[24] H. Soltanian-Zadeh, F. Rafee-Rad and D. Pourabdollah-Nejad, "Comparison of multiwavelet, wavelet, Haralick, and shape features for microcalcifcation classifcation in mammograms", *Pattern Recognition*, vol. 37, pp. 1973–1986, 2004.
[25] D. L. Thiele, C. Kimme-Smith, T. D. Johnson, M. McCombs and L. W. Bassett, "Using tissue texture surrounding calcification clusters to predict benign vs malignant outcomes", *Med. Phys*., vol. 23, pp. 549-555, 1996.
[26] M. Heath, K. Bowyer, D. Kopans, R. Moore, P. Kegelmeyer, "The digital database for screening mammography", in Proc. *5th Int. Workshop on Digital Mammography*, IWDM, Toronto, Canada, 2000, pp. 212-218.
[27] American College of Radiology (1998), Illustrated Breast Imaging Reporting and Data System (BI-RADS), American College of Radiology, third edition.
[28] P. Sakellaropoulos, L. Costaridou and G. Panayiotakis, "A wavelet-based spatially adaptive method for mammographic contrast enhancement", *Phys. Med. Biol.*, vol. 48, pp. 787-803, 2003.
[29] L. Costaridou, P. Sakellaropoulos, S. Skiadopoulos and G. Panayiotakis, "Locally adaptive wavelet contrast enhancement", in *Medical Image Analysis Methods*, L. Costaridou, Ed. Taylor & Francis Group LCC, CRC Press, Boca Raton, FL., 2005, pp. 225-270.
[30] L. Costaridou, S. Skiadopoulos, A. Karahaliou, P. Sakellaropoulos, and G. Panayiotakis, "On the lesion specific enhancement hypothesis in mammography", in *Proc. 14th International Conference of Medical Physics*, ICMP, Nuremberg, Germany, 2005, pp. 949-950.
[31] R. C. Gonzalez, and R. E. Woods, *Digital Image Processing*, Prentice-Hall, Inc., New Jersey, 2002, pp. 76-142.
[32] R. M. Haralick, K. Shanmugam and I. Dinstein, "Textural features for image classification", *IEEE Trans. System Man. Cybernetics*, vol. SMC-3, pp. 610–621, 1973.
[33] R. F. Walker, P. Jackway, and I. D. Longstaff, "Improving co-occurrence matrix feature discrimination", in *Proc. 3rd Conference on Digital Image Computing: Techniques and Applications (DICTA'95)*, Brisbane, Australia, 1995, pp. 643-648.
[34] M. Galloway, "Texture analysis using gray level run lengths", *Comput. Graphics Image Proc.*, vol. 4, pp. 172-179, 1975.
[35] K. I. Laws, "Texture energy measures", in *Proc. DARPA Image Understanding Workshop*, Los Angeles, 1979, pp. 47-51.
[36] S. A. Dudani, "The distance weighted nearest neighbor rule", *IEEE Trans. System Man. Cybernetics*, vol. SMC-6, pp. 325-327, 1976.
[37] G. Ursin, L. Hovanessian-Larsen, Y. R. Parisky, M. C. Pike, and A. H. Wu, "Greatly increased occurrence of breast cancers in areas of mammographically dense tissue", *Breast Cancer Research*, vol. 7, pp. R605-R608, 2005.
[38] H. D. Cheng, X. Cai, X. Chen, L. Hu, X. Lou, "Computer-aided detection and classification of microcalcifications in mammograms: a survey", *Pattern Recognit*., vol. 36, pp. 2967-2991, 2003.
[39] E. Sakka, A. Prentza, D. Koutsouris, "Classification algorithms for microcalcifications in mammograms (Review)", *Oncol. Rep.*, vol. 15(spec no), pp. 1049-1056, 2006.
[40] W. J. H. Veldkamp, N. Karssemeijer, "Influence of segmentation on classification of microcalcifications in digital mammography", in *Proc. 18th Annual International Conference of IEEE Engineering in Medicine and Biology Society*, Amsterdam, Netherlands, 1996, pp. 1171-1172.
[41] S. Paquerault, L. M. Yarusso, J. Papaioannou, Y. Jiang, R. M. Nishikawa, "Radial gradient-based segmentation of mammographic microcalcifications: Observer evaluation and effect on CAD performance", *Med. Phys.*, vol.31, pp. 2648-2657, 2004.

TABLE I
BEST SUBSET OF FEATURES FOR THE FOUR CATEGORIES OF TEXTURAL FEATURES STUDIED AND PERFORMANCE ACHIEVED IN TERMS OF SENSITIVITY, SPECIFICITY AND OVERALL ACCURACY

Feature category	Best Features		Sensitivity (%)	Specificity (%)	Accuracy (%)
FOS	Mean value of grey level Skewness	(k=5)	92.59	63.04	79
GLCM	Mean of Difference Entropy Range of Local Homogeneity Range of Difference Variance	(k=5)	85.18	78.26	82
GLRLM	Mean of SRE Mean of LRE Mean of RPERC	(k=3)	72.22	52.17	63
LTEM	Skewness from S5L5 Mean from R5L5 Mean from L5L5 STD from S5L5 STD from W5L5	(k=5)	90.74	86.96	89

k = number of neighbors.